IEEE Access
Multidisciplinary | Rapid Review | Open Access Journal

Received April 10, 2020, accepted April 26, 2020, date of publication April 29, 2020, date of current version May 15, 2020.

Digital Object Identifier 10.1109/ACCESS.2020.2991331

Temperature Tunable Narrow-Band Terahertz Metasurface Absorber Based on InSb Micro-Cylinder Arrays for Enhanced Sensing Application

FU CHEN, YONGZHI CHENG, AND HUI LUO
School of Information Science and Engineering, Wuhan University of Science and Technology, Wuhan 430081, China

Corresponding author: Yongzhi Cheng (chengyz@wust.edu.cn)

This work was supported in part by the National Natural Science Foundation of China under Grant 61801186 and Grant 61701185, and in part by the Science and Technology Research Project of Education Department of Hubei China under Grant D20181107.

ABSTRACT A narrow-band metasurface absorber (MSA) based on InSb micro-cylinder arrays has been proposed and investigated numerically, which could be believed to be applicable for both temperature and refractive index (RI) sensing in terahertz (THz) region. Distinct from previous designs, the proposed narrow-band MSA is only consisted of a sub-wavelength periodic micro-cylinder array based on the InSb material possessing an extremely thermosensitive relative permittivity which varies with the external environment temperature, and a gold ground-plane deposited on a glass substrate. Numerical simulation results indicate that the proposed MSA can achieve an absorbance of 99.9% at 1.8985 THz and the corresponding Q-factor is about 120.9 at room temperature (300 K). It is inferred that the narrow-band perfect absorption of the MSA could be contributed to the surface plasmon polariton (SPP) resonance mode excitation. Furthermore, the absorption property of the designed MSA is found to be highly sensitive to the RI value variations of the surrounding mediums and fluctuations of external environment temperature. Thus, the proposed MSA can be not only operated as a temperature sensor with a sensitivity of 2.13 GHz/K, but also a RI sensor with a sensitivity of 960 GHz/RIU (refractive index unit). Due to its high sensing performance, it can be believed that the narrow-band MSA has great potential applications in chemical, biological or other optoelectronic related areas.

INDEX TERMS Metasurface absorber, narrow-band, InSb, terahertz region, sensing.

I. INTRODUCTION

Electromagnetic (EM) metamaterial absorber (MMA) is always composed of a periodic array of sub-wavelength resonator structures, which can absorb the light radiation impinged upon it at a particular frequency range [1], [2]. The MMA is typically composed of a three-layers structure in the EM wave's propagation direction, including a micro-/nano-fabricated patterned metallic structure, a dielectric spacer and a metallic ground plane [1]. The perfect EM absorption performance of MMA could be achieved by the reflection minimization via matching the impedance to free-space and the transmission suppression via applying a ground plane simultaneously. In past decade, there has been a tremendous interest in the development of high performance MMA ranging from microwaves to optical frequencies, due to its potential application prospects in modern science and technology areas [2]–[14]. In particularly, the MMA operated in the terahertz (THz) region has attracted increasing attention due to its exciting applications in thermal emitter, imaging, communications, stealth, and sensing [3]–[5], [15]–[27]. What is more, the sensing application of MMA has a growing application potential which is benefitted from THz technology. Generally, typical MMA for RI sensing application in THz region is always based on the metal-dielectric-metal (MDM) structure [19]–[26]. Among these MDM structural MMAs, it is believed that the intermediate dielectric layer could provide a space to accommodate the enhanced EM fields

The associate editor coordinating the review of this manuscript and approving it for publication was Rahul A. Trivedi.

originated from surface plasmon polariton (SPP), localized surface plasmon (LSP) resonances or Fabry-Perot resonances etc. [16]–[20].

Many efforts have been made by several research groups to enhance the absorption capacity of MMAs applied in THz sensing applications [19]–[26]. For example, Yahiaoui et.al., proposed and demonstrated a multichannel THz MMA which can be applied as a refractive index (RI) sensor with a maximum sensitivity of about 139.2 GHz/RIU (refractive index unit) [21]. Geng et.al., proposed an ultra-narrow band MMA with a maximum sensitivity of about 190.4 GHz/RIU [23]. However, the MMA-based sensors mentioned above are still suffered from the relatively complex fabrication and very limited sensitivity, which extremely restrict it from practical application. Besides, it has been also established that many kinds of analytes, such as gas and liquid, are turned out to be in difficulty of bonding with the mentioned MMAs above. Metasurface, as a sub-class of metamaterials, could provide another approach which possesses advantages of higher quality factor, lower profile, and thinner thickness etc. Metasurface is usually consisted of patterned all-dielectric, all-metal or dielectric-metal hybrid patterned structures, which could be used to construct the miniaturized and integrated THz devices due to its quasi-two-dimensional (quasi-2D) planar feature [28]–[33]. Recently, THz metasurface absorbers (MSAs) have been investigated intensively for various applications, which have been confirmed that a perfect absorption performance can be achieved by a relatively simple geometric structure design [29]–[34]. Thus, it also inspires us to design a narrow-band THz MSA with higher quality factor for sensing application.

In this work, we have proposed a temperature tunable narrow-band MSA based on the thermosensitive semiconductor material InSb with an environment temperature dependent relative permittivity, which could be functioned as the temperature and refractive index (RI) sensor simultaneously in THz region. The unit-cell of the proposed MSA is only consisted of a sub-wavelength InSb micro-cylinder array structure and a gold ground-plane placed on a substrate. At room temperature (300 K), it has been confirmed that the proposed MSA exhibited a perfect absorbance of 99.9% at 1.8985 THz and a corresponding high Q-factor of about 120.9. The origin of perfect absorption effect in MSA has been illustrated by analyzing the distributions of electric field and power loss density. Furthermore, the absorption properties of the MSA have been studied systematically by changing the geometric parameters of the InSb micro-cylinder structure. Since the absorption frequency is highly dependent on the external environment temperature and RI value of the surrounding medium, the MSA can be operated as a temperature sensor with a sensitivity of 2.13 GHz/K, and a RI sensor with a sensitivity of 960 GHz/RIU. Relying on its satisfying sensing performance, the narrow-band MSA could be believed to be possessing great potential applications in chemical and biological or other optoelectronic related areas.

II. DESIGN, SIMULATION, EXPERIMENT, AND THEORY

In this section, the electrical properties of the semiconductor material InSb have been firstly studied. It has been well known that the InSb has some advantages, such as low loss, high electron-mobility, temperature-dependent narrow bandgap, low electron density and effective mass in the THz region [35]–[41]. The complex permittivity of semiconductor InSb can be adjusted actively by varying the external environment temperature. In THz region, the complex permittivity of the InSb can be approximately described by the Drude model [35]–[37]:

$$\varepsilon(\omega) = \varepsilon_\infty - \frac{\omega_p^2}{\omega^2 + i\omega\gamma} \tag{1}$$

where ε_∞ is the high-frequency dielectric constant, ω is the angular frequency, ω_p is the plasma frequency, and γ is the damping constant. The plasma frequency is defined as $\omega_p = \sqrt{Ne^2/\varepsilon_0 m^*}$, in which N, e, ε_0 and the m^* is the intrinsic carrier concentration, electronic charge, permittivity of vacuum, and effective mass of the free carries, respectively. The damping constant γ has been confirmed to be proportional to the electron mobility μ, which could be calculated by $\gamma = e/(\mathrm{m}^* \cdot \mu)$. The electron mobility μ in THz region changes slightly when the temperature T (in Kelvin) varies from 295 K to 320 K. Thus, the damping constant γ can be assumed reasonably as a constant of 0.1π THz, which is in well consistent with the experiment data [35]. Other parameters of InSb are given as follows: $\varepsilon_\infty = 15.6$, and $m^* = 0.015m_e = 1.37 \times 10^{-32}$ kg (m_e is electron mass) [41]. It has been also confirmed that the carrier concentration N of semiconductor InSb is highly dependent on the external environment temperature, and it can be described by the formula $N = 5.76 \times 10^{20} T^{1.5} e^{-0.13/k_B T}$, which is in consistent with the reported experimental data as well [36], [37], where k_B, T is the Boltzmann constant and temperature, respectively. Thus, the change of temperature T will directly lead to the variation of the plasma frequency ω_p. Consequently, the $\varepsilon\omega$ of semiconductor InSb is turned out to be dependent on the variation of environment temperature T.

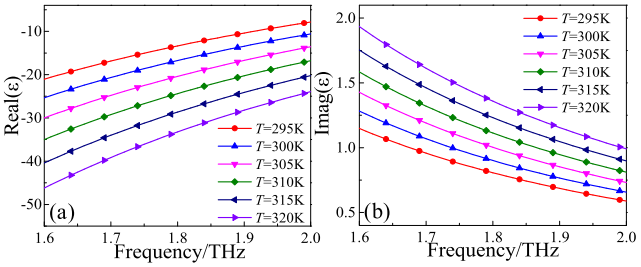

FIGURE 1. The (a) real and (b) imaginary part of calculated relative permittivity $\varepsilon(\omega)$ of the semiconductor material InSb under different external environment temperature T.

Figure 1 presents the calculated real and imaginary parts of complex permittivity $\varepsilon\omega$ of the semiconductor InSb under

different environment temperature T varying from 295 K to 320 K by a step of 5 K. It can be observed that the absolute magnitudes of both real and imaginary parts of the $\varepsilon\omega$ of the InSb increase with the gradually rising temperature T, while the frequency dispersions characteristic remain constant. In particularly, the real part of the $\varepsilon\omega$ is always negative in the entire interested frequency range (1.6 - 2 THz) even under different temperature T, which means that the excitation of plasmonic resonance mode could be easily obtained through the special structural design of the InSb for the normal incident THz wave.

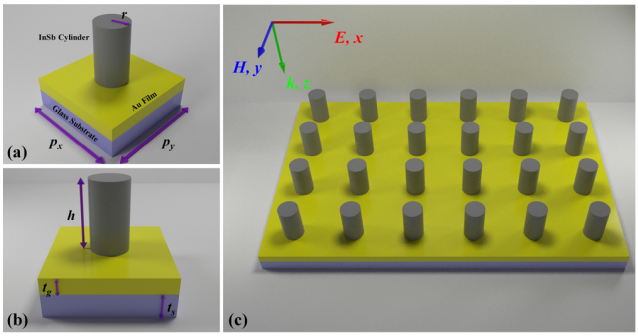

FIGURE 2. Schematic of the proposed temperate tunable narrow-band MSA: (a, b) the axonometric and side views of the unit-cell structure, (c) the quasi-2D array structure.

Due to its excellent optoelectronic properties, the InSb is always used to construct the various temperature tunable THz devices with high performance, which have been demonstrated numerically and experimentally [24], [36]–[43]. Thus, it inspires us to design the proposed temperature tunable narrow-band THz MSA as well, as shown in Fig. 2. In this design, the semiconductor InSb was selected to construct the surface plasmonic resonator unit of proposed MSA, whose complex permittivity in THz region can be tuned dynamically by adjusting the external environment temperature. As shown in Fig. 2(a), the elementary building block of the unit-cell in the MSA only consists of single InSb based micro-cylinder structure adhered on a continuous gold film. In this design, as illustrated in Fig. 2(b), a 20 μ thickness continuous gold film has been chosen as the mirror reflector deposited on a glass substrate. Besides, the quasi-2D periodical array structure of the designed MSA was arranged in the x- and y-axis directions, as depicted in Fig. 2(c). Since the incident THz waves can be easily guided and concentrated by the proposed MSA, the EM filed can be consequently significantly enhanced in the edge of InSb micro-cylinder structure. In addition, owing to the special microstructure design in this work, it can be believed that proposed MSA exhibits a better infiltration and diffusion effects of analyte which is superior to previous reported MDM structures [7]–[10], [16]–[18], [15]–[25]. The incident THz plane wave with x-direction polarization was set to propagate alone the z direction which is vertical to the periodic structure surface of proposed MSA. In this configuration, it can be reasonably expected the excitation of LSP or SPP resonance mode in the InSb micro-cylinder structure since the real part of its permittivity is negative in our interested frequency range (1.6 - 2 THz) [40]–[43].

To efficiently investigate the proposed MSA, the three-dimensional (3D) finite element method (FEM) simulations have been performed by using CST Microwave Studio. In simulations, a broadband linear polarization plane wave was set to irradiate perpendicularly to the unit-cell structure of the proposed MSA along the $+z$ direction. In addition, the periodic boundary conditions (along the x- and y-axis directions) have been also applied for the transverse boundaries to replicate an infinite array of the InSb micro-cylinder structures. The conductivity of gold ground-plane is reasonably set to be 4.56×10^7 S/m at a temperature of 300 K. The optimized geometrical parameters are given as follows: $p_x = p_y = 150\ \mu$m, $r = 25\mu$m, $h = 89\ \mu$m, $t_s = 30\mu$m, $t_g = 20\ \mu$m. The thickness of the gold ground-plane is much larger than the typical skin depth in THz regime, thus the transmission of incident waves can be effectively suppressed. Hence, the absorbance can be simply expressed as $A(\omega) = 1 - R(\omega) = 1 - S_{11}(\omega)|^2$, where $S_{11}(\omega)$ represents the reflection coefficient as functions of frequency ω.

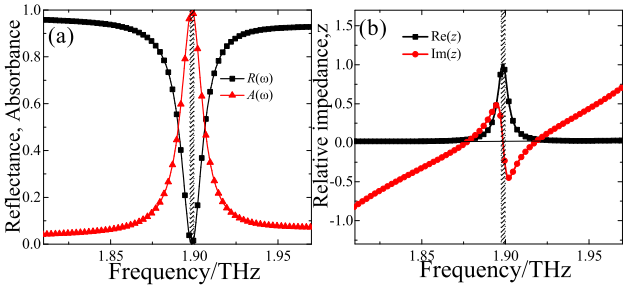

FIGURE 3. (a) Simulated reflectance ($R(\omega)$, black line) and absorbance ($A(\omega)$, red line) spectra of proposed MSA at a temperature of 300 K, (b) the corresponding relative wave impedance.

III. RESULTS AND DISCUSSION

The simulated reflectance ($R(\omega)$) and absorbance ($A(\omega)$) spectra of the proposed MSA at a temperature of 300 K have been illustrated in Fig. 3(a). A narrow and sharp trough of reflection at 1.8985 THz has been observed evidently, and the minimum reflectance is found to be as low as 0.01% whereas the corresponding absorbance reaches up to 99.99%. Besides, it can be also expected that the designed MSA is polarization insensitive for both TE and TM modes under normal incidence due to its high geometric rotation symmetry of the unit-cell structure. In order to further reveal the narrow-band perfect absorption properties, the FWHM (full-width at half maximum) and Q-factor of the proposed MSA have been also calculated and analyzed. The FWHM bandwidth of the resonance absorption peak is only about 0.0157 THz, and the Q-factor of the proposed MSA is about 120.9, which

is obviously superior to the previous designs [5], [20]–[22]. Hence, it can be reasonably believed that the proposed MSA exhibiting such sharp resonance absorption peak possesses great application potential in high sensitivity sensing field owing to the ultra-narrow FWHM and high Q-factor [19]–[25]. In other words, it signifies that the proposed MSA could effectively and sensitively response to a subtle RI value variation of surrounding analyst in terms of an evidently observable shift of the resonance absorption peak. In order to investigate the physical mechanisms of the observed perfect absorption phenomenon, the relative wave impedance of proposed MSA has been also calculated by extracting the simulated reflection coefficient S_{11} based on the S-parameter retrieved method [44], [45]. As shown in Fig. 3(b), it can be found that the imaginary part of relative impedance is close to zero (Im(z) $\approx$ 0), while the real part approaches to the maximum value which is near-unity (Re(z) $\approx$ 1) at the resonance frequency of 1.8985 THz. Thus, the reflection of proposed MSA could be consequently suppressed to nearly zero since the relative wave impedance of the proposed MSA is almost matched to the free space ($z_0 \approx 1$) at resonance frequency.

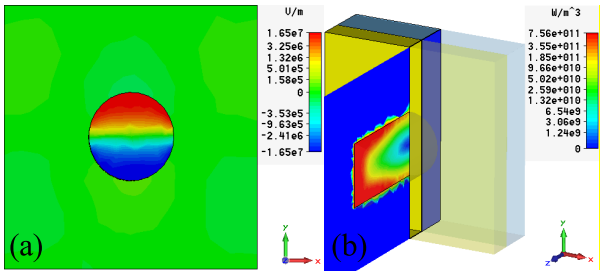

FIGURE 4. Distributions of the electric field E_z (in the x–y plane) and (b) power loss density (in the y–z plane) of the middle plane of the unit-cell structure in the proposed MSA at 1.8985 THz at a temperature of 300 K.

To further reveal the physical origin of the perfect absorption phenomenon in proposed MSA, the distributions of electric field and power loss density at a temperature of 300 K have been systematically studied. Figure 4(a) illustrates the z-component (E_z) distribution of the induced electric field at resonance frequency of 1.8985 THz. In comparison, the InSb micro-cylinder structure has an obvious advantage that it could couple directly with not only the electric field but also the magnetic field of the normal incident wave [25]–[27]. According to the top view of MSA as shown in Fig.4 (a), it can be recognized that the localized z-component of electric field (E_z) is strongly concentrated and enhanced in the upper and down surface and edge of the InSb micro-cylinder structure along the y-axis direction. In addition, the blue and red regions in the InSb micro-cylinder structure indicate the distributions of the induced negative and opposite charges under normal incident THz wave illumination, respectively. The accumulations of the negative and positive charges in the InSb micro-cylinder structure reveal that the perfect absorption of MSA is originated from the excitation of the fundamental dipolar mode, which is consistent with the natural of the SPP resonance mode. Thus, such a spatial field feature indicates that the formation of SPP resonance mode can be believed to be originated from the excitation of strong near-field coupling between the air and InSb micro-cylinder structure [40]–[43].

Figure 4(b) depicts the distribution of power loss density in the middle plane (in the y–z plane) of the unit-cell structure at the resonance frequency 1.8985 THz when the environment temperature is set to be 300 K. It is evident that the power loss density is concentrated on the inner of the InSb micro-cylinder structure, and it decays gradually with the transmission of incident THz waves. It can be also found that the energy of incident THz wave is significantly enhanced at the InSb-Au interface of the MSA due to the excitation of the SPP resonance mode. Accordingly, it can be believed that the energy loss of incident THz waves, which is induced by the excitation of SPP resonance mode in the designed InSb micro-cylinder structure dielectric resonator, is large enough to enhance the perfect absorption at resonance. Due to the enhanced field distribution of InSb micro-cylinder structure, the energy of incident waves can be efficiently confined in the inner of the InSb micro-cylinder structure and no waves can thus be reflected back. In addition, it can be also expected that the periodic structured semiconductor InSb material may also acts as an effective absorber and consequently contributes to the perfect absorption of the proposed MSA owing to its dielectric loss feature in THz region. It should be noticed that the incident wave would be strongly repulsed by continuous gold film in THz region, and the perfect absorption cannot be possible without the SPP resonance excited in the InSb micro-cylinder structure. Hence, it further confirms that the SPP resonance in the InSb micro-cylinder structure makes great contribution to the high absorption of the MSA. It means that the InSb micro-cylinder structure enables the enhanced THz wave transmission through the SPP mode, while the transmitted THz wave could be strongly coupled and extremely absorbed at the interface between the InSb micro-cylinder structure and continuous gold film. Consequently, it can be concluded that the excitation of SPP resonance mode and intrinsic dielectric loss of the InSb micro-cylinder structure are the two critical factors to achieve the high absorption of the designed MSA.

Additionally, it is necessary to investigate the influence of geometric parameters on the absorption capacity of the proposed MSA. Here, owing to the simplified construction of the MSA, only two geometric parameters of the InSb micro-cylinder need to be considered: the radius r and height h, respectively. The absorbance spectra with different r and h of the InSb micro-cylinder structure at a temperature of 300 K have been illustrated in Fig. 5. According to the Fig. 5(a), it can be observed that the absorption amplitude of the proposed MSA almost remains constant when the radius r of InSb micro-cylinder structure gradually increases from

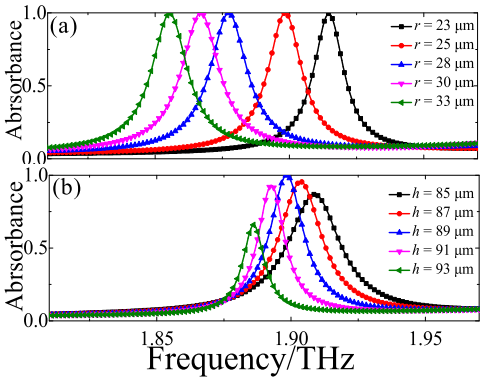

FIGURE 5. The absorbance spectra of the proposed MSA with different (a) radius *r*, and (b) height *h* of the InSb micro-cylinder structure at a temperature of 300 K.

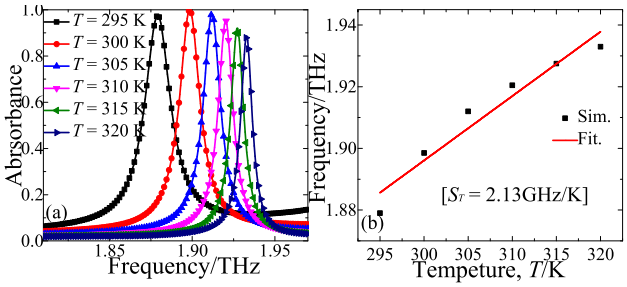

FIGURE 6. (a) The absorbance spectra of the MSA-based temperature sensor by changing the surrounding environment temperature *T*, (b) the simulated resonance frequency (square symbols) and linear fit (solid line) and as a function of the external environment temperature.

23 μm to 33 μm, whereas an evidently obvious red-shift of the resonance peak has been detected simultaneously. In other words, it can be concluded that the resonance absorption frequency of the MSA is nearly inverse proportional to r, which could be explained by the LC model according to the equivalent circuit theory [46]. In the LC model, the resonance absorption frequency of the MSA can be approximately given as $f_0 = 1/(2\pi\sqrt{LC}) \propto 1/(r \cdot \sqrt{\varepsilon_r \cdot h})$, where ε_r, r and h is the relative permittivity, radius and height of the InSb micro-cylinder structure, respectively. Obviously, the resonance absorption frequency would gradually decrease with the enlarged radius r due to the increase of the equivalent inductance L. On the other hand, Figure 5(b) depicts the absorbance spectra of proposed MSA which is consisted of InSb micro-cylinder structure with various height (h = 85 μm, 87 μm, 89 μm, 91 μm, and 93 μm). In this case, the absorption amplitude of proposed MSA exhibits a non-monotonic variation trend which is firstly increased and then gradually decreased, while the corresponding absorption frequency is slightly red shifted with the increasing h which can be also confirmed by the LC model. Evidently, it can be found that the absorbance of proposed MSA could achieve the maximum when the height of InSb micro-cylinder is set to be the optimized value $h = 89$ μm. Thus, it can be concluded that the absorption properties of the proposed MSA can be adjusted dynamically by changing the geometrical parameters of the InSb micro-cylinder structure.

As outlined and discussed earlier, the semiconductor InSb is a temperature-sensitive material, whose complex permittivity will vary with the fluctuation of the external environment temperature. Thus, it is reasonably considered that the designed MSA based on InSb micro-cylinder structure has a potential application in temperature sensing area. Figure 6(a) illustrates the absorbance spectra of the proposed MSA under different external environment temperature (T = 295 K, 300 K, 305 K, 310 K, 315 K, and 320 K). It can be seen that the absorbance of the MSA is first slightly increased and then gradually decreased, while the corresponding resonance absorption frequency exhibits an obvious blue-shift with the increase of T. It could be inferred that the minor variation of the absorbance of the MSA is mainly originated from the slight dielectric loss variation of the semiconductor material InSb under different environment temperature. Furthermore, it needs to be emphasized that the absorbance of proposed MSA always remains over 90% in the whole temperature range from 295 K to 320 K. Besides, according to the LC model, it can be also concluded that the inverse relation between environment temperature T and absolute value of relative permittivity ε_r of semiconductor InSb (as shown in Fig. 1) should be responsible for the obvious blue-shift of the resonance absorption frequency.

To evaluate the temperature sensing performance of the MSA-based sensor, we further define a key indicator which is the temperature sensitivity. The temperature sensitivity S_T is defined as the resonance absorption frequency shift Δf caused by a certain permittivity variation of the InSb due to the minor change ΔT of the environment temperature. Thus, the temperature sensitivity can be expressed as $S_T = \Delta f/\Delta T$ [24], [43], [45], whose unit is consequently defined as the shift frequency per temperature unit (GHz/K). Figure 6(b) presents the dependent relations between the absorption frequency shift Δf and the temperature variation ΔT of surrounding environment. As shown in Fig. 6(b), the resonance absorption frequency is shifted to the higher frequency region with the increasing temperature which can be further described by an approximate linear relative function between them, shown as the fitted solid line. It can be seen that the slope of the fitting curve actually depicts the changing rate of absorption frequency with temperature, and the value of S_T is about 2.13 GHz/K. Thus, it could be expected that the proposed MSA can be served as a good temperature sensor.

On the other hand, the RI sensing performance of the proposed MSA and the effects of the RI variations on the absorbance spectrum have been also investigated in detail. As shown in Fig. 7(a), the schematic of MSA-based RI sensor has been presented which could be believed as a new route for sensing application of biomedical and chemical molecules.

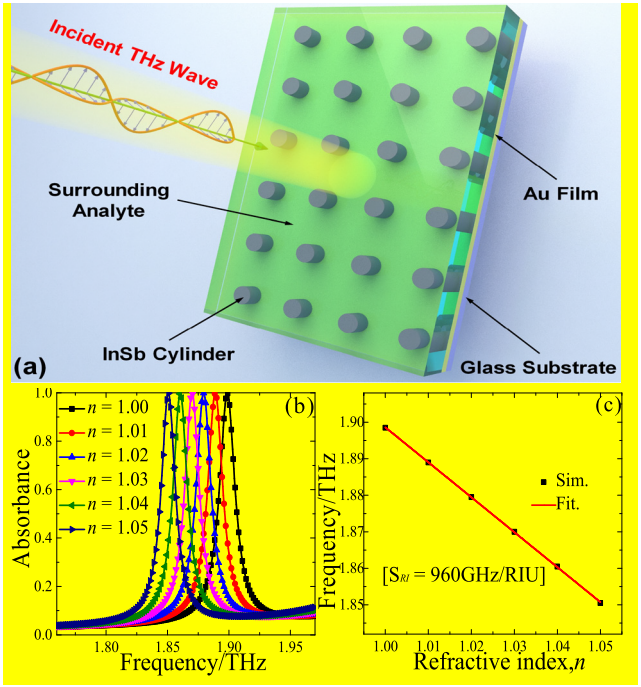

FIGURE 7. (a) The schematic of MSA-based RI sensor, (b) the absorbance spectra of the MSA-based RI sensor by changing the surrounding analyte from air to aqueous glucose solution with different RI values, and (c) the simulated resonance frequency (square symbol) and linear fit (solid line) as a function of RI values of the surrounding analyte.

For evaluating the performance of RI sensing application, the air is assumed as the reference while glucose aqueous solution is accepted as the analyte to be measured, both of which could be evenly and fully diffused in surrounding space around the InSb micro-cylinder structure of the proposed MSA. When RI value of the surrounding analyte slightly varies from 1.00 to 1.05 by a step of 0.01 by controlling the concentration of the glucose aqueous solution, an evidently obvious red-shift of the absorption peak can be easily detected, as shown in Fig. 7(b). It can be identified that the absorption peak frequency of the narrow-band MSA is highly dependent on the RI value of the surrounding analyte. Furthermore, it needs to be noticed that the relative narrow-band FWHM and high Q-factor of proposed MSA could be kept nearly unchanged with the variation of the RI value.

In order to clearly verify the RI sensing performance of the proposed MSA-based sensor, the sensitivity (S_{RI}) and figure of merit (FOM_{RI}) for the proposed MSA have been defined. The S_{RI} has been defined as the resonance absorption frequency shift (Δf) caused by a minor RI change (Δn) of the surrounding analyte. Thus, the RI sensitivity can be expressed as $S_{RI} = \Delta f / \Delta n$, whose unit is always accepted as the shift frequency per refractive index unit (GHz / RIU) [20]–[22]. Besides, another key indicator FOM_{RI} could be considered as the quotient acquired from the S_{RI} divided by the FWHM of resonance absorption peak frequency, which can be expressed as $FOM_{RI} = S_{RI} /$ FWHM [11]. As shown in Fig. 7(c), the relation between the frequency shift Δf of the absorption peak and the variation of RI value (Δn) of the surrounding analyte has been distinctly depicted. According to the fitting result, it is evident that the resonance frequency of the proposed MSA decrease almost linearly with the increasing RI of the surrounding analyte since the fitting solid line comes through all the resonance frequency points. Furthermore, it can be also clarified that the bulk RI sensitivity S_{RI} is about 960 GHz/RIU which is obviously superior to previous designed sensors operated in THz region [5], [20]–[22]. Since the frequency FWHM of the proposed MSA structure surrounded by air is about 15.8 GHz, the corresponding FOM_{RI} could be calculated to be about 60.76 according to the definition mentioned above. Thus, it could be believed that these excellent characteristics of the proposed MSA would provide effective guides for the design of high sensitivity RI sensor in THz region.

IV. CONCLUSIONS

In conclusion, we present a simple and effective design of the tunable narrow-band MSA based on InSb micro-cylinder structure array in THz region, which could be functioned as temperature and RI sensor simultaneously. The numerical simulation result indicates that the proposed MSA can achieve an extremely high absorbance of 99.9% and a corresponding Q-factor of about 120.9 at 1.8985 THz under the room temperature (300 K). The distribution of the enhanced electric field reveals that the narrow-band absorption is originated from the excitation of the SPP resonance mode. Besides, the distribution of the power loss density further confirms that the dielectric loss feature of semiconductor material InSb in THz region is also a critical factor for the perfect absorption of the MSA. In addition, it has been also verified that the absorption performance of proposed MSA would be strongly affected by the variation of geometric parameters of InSb micro-cylinder structure. The further simulation results indicate that the designed MSA exhibits a highly sensitive response to the external environment temperature and RI change of surrounding analyte simultaneously. Numerical results manifest that the proposed MSA could achieve a sensitivity of about 2.13 GHz/K when it serves as a temperature sensor, while a high sensitivity of 960 GHz/RIU and corresponding FOM of about 60.76 can be also acquired when it functions as a RI sensor. Owing to its high sensing performance above, it is reasonably believed that our design could be an alternative effective approach for achieving high-quality multifunction sensor for biotechnology, medical diagnostics, gas/liquid detection, and spatial biosensing.

REFERENCES

[1] C. M. Watts, X. Liu, and W. J. Padilla, "Metamaterial electromagnetic wave absorbers," *Adv. Mater.*, vol. 24, no. 23, pp. 98–120, Jun. 2012.
[2] Y. Cheng, Y. Zou, H. Luo, F. Chen, and X. Mao, "Compact ultra-thin seven-band microwave metamaterial absorber based on a single resonator structure," *J. Electron. Mater.*, vol. 48, no. 6, pp. 3939–3946, Jun. 2019.
[3] M. Diem, T. Koschny, and C. M. Soukoulis, "Wide-angle perfect absorber/thermal emitter in the terahertz regime," *Phys. Rev. B, Condens. Matter*, vol. 79, no. 3, Jan. 2009, Art. no. 033101.

[4] K. Iwaszczuk, A. C. Strikwerda, K. Fan, X. Zhang, R. D. Averitt, and P. U. Jepsen, "Flexible metamaterial absorbers for stealth applications at terahertz frequencies," *Opt. Express*, vol. 20, no. 1, p. 635, Jan. 2012.

[5] B.-X. Wang, G.-Z. Wang, and T. Sang, "Simple design of novel triple-band terahertz metamaterial absorber for sensing application," *J. Phys. D, Appl. Phys.*, vol. 49, no. 16, Apr. 2016, Art. no. 165307.

[6] N. Liu, M. Mesch, T. Weiss, M. Hentschel, and H. Giessen, "Infrared perfect absorber and its application as plasmonic sensor," *Nano Lett.*, vol. 10, no. 7, pp. 2342–2348, Jul. 2010.

[7] C. Cen, Z. Yi, G. Zhang, Y. Zhang, C. Liang, X. Chen, Y. Tang, X. Ye, Y. Yi, J. Wang, and J. Hua, "Theoretical design of a triple-band perfect metamaterial absorber in the THz frequency range," *Results Phys.*, vol. 14, Sep. 2019, Art. no. 102463.

[8] Y. Z. Cheng, X. Zuo, M. L. Huang, T. Wang, and R. Gong, "Design of a photo-excited broadband tunable terahertz absorber," *J. Infr. Millim. Waves*, vol. 38, no. 1, pp. 97–102, 2019.

[9] A. Sobhani, M. W. Knight, Y. Wang, B. Zheng, N. S. King, L. V. Brown, Z. Fang, P. Nordlander, and N. J. Halas, "Narrowband photodetection in the near-infrared with a plasmon-induced hot electron device," *Nature Commun.*, vol. 4, no. 1, p. 1643, Jun. 2013.

[10] Y. Wang, Z. Chen, D. Xu, Z. Yi, X. Chen, J. Chen, Y. Tang, P. Wu, G. Li, and Y. Yi, "Triple-band perfect metamaterial absorber with good operating angle polarization tolerance based on split ring arrays," *Results Phys.*, vol. 16, Mar. 2020, Art. no. 102951.

[11] Y. Cheng, H. Luo, F. Chen, and R. Gong, "Triple narrow-band plasmonic perfect absorber for refractive index sensing applications of optical frequency," *OSA Continuum*, vol. 2, no. 7, p. 2113, Jul. 2019.

[12] J. Li, X. Chen, Z. Yi, H. Yang, Y. Tang, Y. Yi, W. Yao, J. Wang, and Y. Yi, "Broadband solar energy absorber based on monolayer molybdenum disulfide using tungsten elliptical arrays," *Mater. Today Energy*, vol. 16, Jun. 2020, Art. no. 100390.

[13] Y. Cheng and C. Du, "Broadband plasmonic absorber based on all silicon nanostructure resonators in visible region," *Opt. Mater.*, vol. 98, Dec. 2019, Art. no. 109441.

[14] J. Li, Z. Chen, H. Yang, Z. Yi, X. Chen, W. Yao, T. Duan, P. Wu, G. Li, and Y. Yi, "Tunable broadband solar energy absorber based on monolayer transition metal dichalcogenides materials using au nanocubes," *Nanomaterials*, vol. 10, no. 2, p. 257, 2020.

[15] I. Escorcia Carranza, J. P. Grant, J. Gough, and D. Cumming, "Terahertz metamaterial absorbers implemented in CMOS technology for imaging applications: Scaling to large format focal plane arrays," *IEEE J. Sel. Topics Quantum Electron.*, vol. 23, no. 4, Jul. 2017, Art. no. 4700508.

[16] L. Huang, D. R. Chowdhury, S. Ramani, M. T. Reiten, S.-N. Luo, A. J. Taylor, and H.-T. Chen, "Experimental demonstration of terahertz metamaterial absorbers with a broad and flat high absorption band," *Opt. Lett.*, vol. 37, no. 2, p. 154, Jan. 2012.

[17] M. Huang, Y. Cheng, Z. Cheng, H. Chen, X. Mao, and R. Gong, "Design of a broadband tunable terahertz metamaterial absorber based on complementary structural graphene," *Materials*, vol. 11, no. 4, p. 540, 2018.

[18] F. Chen, Y. Cheng, and H. Luo, "A broadband tunable terahertz metamaterial absorber based on single-layer complementary gammadion-shaped graphene," *Materials*, vol. 13, no. 4, p. 860, 2020.

[19] K. A. Willets and R. P. Van Duyne, "Localized surface plasmon resonance spectroscopy and sensing," *Annu. Rev. Phys. Chem.*, vol. 58, pp. 267–297, May 2007.

[20] L. Cong, S. Tan, R. Yahiaoui, F. Yan, W. Zhang, and R. Singh, "Experimental demonstration of ultrasensitive sensing with terahertz metamaterial absorbers: A comparison with the metasurfaces," *Appl. Phys. Lett.*, vol. 106, no. 3, Jan. 2015, Art. no. 031107.

[21] R. Yahiaoui, S. Tan, L. Cong, R. Singh, F. Yan, and W. Zhang, "Multispectral terahertz sensing with highly flexible ultrathin metamaterial absorber," *J. Appl. Phys.*, vol. 118, no. 8, Aug. 2015, Art. no. 083103.

[22] H. Zhou, C. Yang, D. Hu, D. Li, X. Hui, F. Zhang, M. Chen, and X. Mu, "Terahertz biosensing based on bi-layer metamaterial absorbers toward ultra-high sensitivity and simple fabrication," *Appl. Phys. Lett.*, vol. 115, no. 14, Sep. 2019, Art. no. 143507.

[23] Z. Geng, W. Su, X. Wang, Y. Jiang, and Y. Liu, "Numerical design of a metasurface-based ultra-narrow band terahertz perfect absorber with high Q-factors," *Optik*, vol. 194, Oct. 2019, Art. no. 163071.

[24] M. Aslinezhad, "High sensitivity refractive index and temperature sensor based on semiconductor metamaterial perfect absorber in the terahertz band," *Opt. Commun.*, vol. 463, May 2020, Art. no. 125411.

[25] B.-X. Wang, Y. He, P. Lou, and W. Xing, "Design of a dual-band terahertz metamaterial absorber using two identical square patches for sensing application," *Nanosc. Adv.*, vol. 2, no. 2, pp. 763–769, Feb. 2020, doi: 10.1039/c9na00770a.

[26] A. A. Jamali and B. Witzigmann, "Plasmonic perfect absorbers for biosensing applications," *Plasmonics*, vol. 9, no. 6, pp. 1265–1270, Dec. 2014.

[27] M. Wu, X. Zhao, J. Zhang, J. Schalch, G. Duan, K. Cremin, R. D. Averitt, and X. Zhang, "A three-dimensional all-metal terahertz metamaterial perfect absorber," *Appl. Phys. Lett.*, vol. 111, no. 5, Jul. 2017, Art. no. 051101.

[28] M. Chen, D. Zhao, J. Cai, C. Wang, X. Xiao, and L. Chang, "All-dielectric metasurfaces for circularly polarized beam-splitters with high conversion efficiency and broad bandwidth," *Optik*, vol. 165, pp. 41–49, Jul. 2018.

[29] M. A. Cole, D. A. Powell, and I. V. Shadrivov, "Strong terahertz absorption in all-dielectric Huygens' metasurfaces," *Nanotechnology*, vol. 27, no. 42, Oct. 2016, Art. no. 424003.

[30] X. Liu, K. Fan, I. V. Shadrivov, and W. J. Padilla, "Experimental realization of a terahertz all-dielectric metasurface absorber," *Opt. Express*, vol. 25, no. 1, p. 191, Jan. 2017.

[31] K. Fan, J. Y. Suen, X. Liu, and W. J. Padilla, "All-dielectric metasurface absorbers for uncooled terahertz imaging," *Optica*, vol. 4, no. 6, p. 601, Jun. 2017.

[32] J. Gao, C. Lan, Q. Zhao, B. Li, and J. Zhou, "Experimental realization of mie-resonance terahertz absorber by self-assembly method," *Opt. Express*, vol. 26, no. 10, p. 13001, May 2018.

[33] H. Luo and Y. Cheng, "Dual-band terahertz perfect metasurface absorber based on bi-layered all-dielectric resonator structure," *Opt. Mater.*, vol. 96, Oct. 2019, Art. no. 109279.

[34] X. You, A. Upadhyay, Y. Cheng, M. Bhaskaran, S. Sriram, C. Fumeaux, and W. Withayachumnankul, "Ultra-wideband far-infrared absorber based on anisotropically etched doped silicon," *Opt. Lett.*, vol. 45, no. 5, p. 1196, Mar. 2020.

[35] M. Oszwałldowski and M. Zimpel, "Temperature dependence of intrinsic carrier concentration and density of states effective mass of heavy holes in InSb," *J. Phys. Chem. Solids*, vol. 49, no. 10, pp. 1179–1185, Jan. 1988.

[36] P. P. Iyer, M. Pendharkar, C. J. Palmstrøm, and J. A. Schuller, "Ultra-wide thermal free-carrier tuning of dielectric antennas coupled to epsilon-near-zero substrates," *Nature Commun.*, vol. 8, no. 1, p. 472, Dec. 2017.

[37] Q. Mu, F. Fan, S. Chen, S. Xu, C. Xiong, X. Zhang, X. Wang, and S. Chang, "Tunablemagneto-optical polarization device for terahertz waves based on InSb and its plasmonic structure," *Photon. Res.*, vol. 7, pp. 325–331, Mar. 2019.

[38] J. Chen, "Tunable slow light in semiconductor metamaterial in a broad terahertz regime," *J. Appl. Phys.*, vol. 107, no. 9, May 2010, Art. no. 093104.

[39] X. Wang, A. A. Belyanin, S. A. Crooker, D. M. Mittleman, and J. Kono, "Interference-induced terahertz transparency in a semiconductor magneto-plasma," *Nature Phys.*, vol. 6, no. 2, pp. 126–130, Feb. 2010.

[40] J. Zhu, J. Han, Z. Tian, J. Gu, Z. Chen, and W. Zhang, "Thermal broadband tunable terahertz metamaterials," *Opt. Commun.*, vol. 284, no. 12, pp. 3129–3133, Jun. 2011.

[41] W. Li, D. Kuang, F. Fan, S. Chang, and L. Lin, "Subwavelength B-shaped metallic hole array terahertz filter with InSb bar as thermally tunable structure," *Appl. Opt.*, vol. 51, no. 29, p. 7098, Oct. 2012.

[42] N. T. Hien, L. N. Le, P. T. Trang, B. S. Tung, N. D. Viet, P. T. Duyen, N. Manh Thang, D. T. Viet, Y. Lee, V. D. Lam, and N. T. Tung, "Characterizations of a thermo-tunable broadband fishnet metamaterial at THz frequencies," *Comput. Mater. Sci.*, vol. 103, pp. 189–193, Jun. 2015.

[43] H. Zou and Y. Cheng, "Design of a six-band terahertz metamaterial absorber for temperature sensing application," *Opt. Mater.*, vol. 88, pp. 674–679, Feb. 2019.

[44] D. R. Smith, D. C. Vier, T. Koschny, and C. M. Soukoulis, "Electromagnetic parameter retrieval from inhomogeneous metamaterials," *Phys. Rev. E, Stat. Phys. Plasmas Fluids Relat. Interdiscip. Top.*, vol. 71, no. 3, Mar. 2005, Art. no. 036617.

[45] W. Li and Y. Cheng, "Dual-band tunable terahertz perfect metamaterial absorber based on strontium titanate (STO) resonator structure," *Opt. Commun.*, vol. 462, May 2020, Art. no. 125265.

[46] K. Carver and J. Mink, "Microstrip antenna technology," *IEEE Trans. Antennas Propag.*, vol. AP-29, no. 1, pp. 2–24, Jan. 1981.

FU CHEN received the B.S. degree in electronic science and technology, the M.S. degree in integrated circuit engineering, and the Ph.D. degree in microelectronics and solid-state electronics from the Huazhong University of Science and Technology, Wuhan, China, in 2011, 2013, and 2016, respectively. He is currently a Lecturer with the School of Information Science and Engineering, Wuhan University of Science and Technology, Wuhan. His research interests include design and fabrication of infrared stealth materials, synthesis of micro- and nano-microwave absorber, and the fundamental study of static and dynamic magnetic properties of ferrites and alloys.

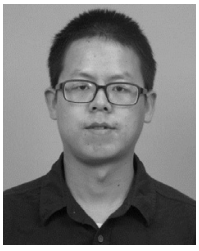

YONGZHI CHENG received the Ph.D. degree in microelectronics and solid state electronics from the Huazhong University of Science and Technology, China, in 2015. He is currently an Associate Professor with the Wuhan University of Science and Technology. His research was in the field of electromagnetic (terahertz, infrared and visible) and physics. For one year, he worked as a Visiting Ph.D. student with the T-Ray Labs, University of Adelaide, where he studied and designed metamaterial plasmonic devices for terahertz waves. His current research interests include areas of electromagnetic (microwave, terahertz, infrared, and visible) and physics, metamaterial or metasurface, and so on.

HUI LUO received the B.S. degree in applied physics from Shangqiu Normal University, Shangqiu, China, in 2011, and the Ph.D. degree in microelectronics and solid-state electronics from the Huazhong University of Science and Technology, Wuhan, China, in 2016. He is currently a Lecturer with the School of Information Science and Engineering, Wuhan University of Science and Technology, Wuhan, China. His research interest includes design and fabrication of micro/nano-absorber and functional structure absorbing material.